

show good agreement with the spectroscopic results.<sup>45</sup> This is a clear indication that the approximation of the CF<sub>3</sub> motion by anisotropic thermal parameters has a negligible effect on the other atomic parameters.

(45) B. Bak, L. Hansen-Nygaard, and J. Rastrup-Anderson, *J. Mol. Spectrosc.*, **2**, 361 (1958).

**Registry No.** Zn(F<sub>6</sub>acac)<sub>2</sub>(py)<sub>2</sub>, 38402-93-6; Cu(F<sub>6</sub>acac)<sub>2</sub>(py)<sub>2</sub>, 38496-50-3.

**Acknowledgments.** This work was supported by the National Science Foundation, Grant GP-11701. Thanks are extended by J. P.-S. to the Lubrizol Foundation for an A. W. Smith Fellowship and to the Colombian Institute "ICFES" for financial support.

Contribution from the Department of Chemistry, Case Western Reserve University, Cleveland, Ohio 44106

## Base Adducts of $\beta$ -Ketoenolates. VI.<sup>1,2</sup> Single-Crystal Electron Paramagnetic Resonance and Optical Studies of Copper(II)-Doped *cis*-Bis(hexafluoroacetylacetonato)bis(pyridine)zinc(II), Cu-Zn(F<sub>6</sub>acac)<sub>2</sub>(py)<sub>2</sub>

J. PRADILLA-SORZANO and JOHN P. FACKLER, Jr.\*

Received August 4, 1972

The epr spectra of Cu(II) doped into Zn(F<sub>6</sub>acac)<sub>2</sub>(py)<sub>2</sub> have been investigated at 4.2°K and in the temperature range 133–300°K. At 4.2°K the spectra are those of three kinds of copper ion, each with approximately axial symmetry about one of the three axes of the octahedron. Two of the epr signals have equal values for their magnetic parameters and intensities. The other, which is the strongest one, corresponds to *g* and hyperfine tensors nearly equivalent to those found at 133°K, with the *z* axis nearly perpendicular to the CuN<sub>2</sub>O<sub>2</sub> plane. Spectra observed above this temperature show that all molecules in the crystal are magnetically equivalent. A temperature dependence has been observed in the spin-Hamiltonian parameters which are weighted averages of the corresponding values for the static configurations found at 4.2°K. The low- and high-temperature epr spectra are interpreted as due to the static and dynamic Jahn-Teller distortions of the complex. A vibronic energy surface, for which one of the three potential energy minima is slightly more favorable than the other two, has been proposed for the copper-doped complex. This nearly degenerate ground state is interpreted as being a consequence of the axial compression that the copper impurity suffers by crystal packing forces. Single-crystal electronic spectra give further support to this interpretation.

### Introduction

The implications of the Jahn-Teller theorem for octahedral inorganic complexes possessing electronically degenerate states have been extensively investigated.<sup>3</sup> Experimental evidence of the theoretical predictions is very often clouded by other concurrent physical effects which can produce the same result as the Jahn-Teller forces. This is particularly true for static distortions which one can attribute to ordinary elastic forces in the crystal or other theoretically acceptable possibilities such as those proposed by Smith<sup>4</sup> for tetragonal Cu(II) and Cr(II) systems.

In contrast to ambiguous illustrations of the Jahn-Teller theorem in structural chemistry, a number of examples have been reported in optical<sup>5,6</sup> and microwave spectroscopy.<sup>7,8</sup> The low-energy band found in the near-infrared region (6–10 kK) has been considered a d-d transition in nearly octahedral Cu(II),<sup>5,9,10</sup> Cr(II), and Mn(III)<sup>6</sup> complexes. This assignment is in accord with predictions of

Liehr and Ballhausen,<sup>11</sup> who showed that a Jahn-Teller distortion can result in the splitting of the E<sub>g</sub> octahedral degeneracy of about 7.0 kK. Transitions between branches of the E ground state, in complexes for which a regular octahedral configuration has been found, have been interpreted as due to dynamic Jahn-Teller distortions.<sup>6</sup> Complexes having an orbital doublet ground state, such as d<sup>9</sup> and low-spin d<sup>7</sup> octahedral ions, have provided most investigations of Jahn-Teller effects by epr methods. Transitions between high-temperature isotropic to low-temperature anisotropic epr spectra<sup>12,13</sup> have been observed for Cu(II) in octahedral environments. O'Brien<sup>14</sup> has provided the theory for strong vibronic coupling and analyzed the dynamic effects resulting when the complex oscillates between the energy minima corresponding to equivalent elongations along the axes of the octahedron.

For those six-coordinate complexes in which the symmetry of the crystal field is obviously lower than trigonal, one cannot rigorously attribute static distortions or fluxional behavior to the Jahn-Teller theorem. However, because ground-state degeneracy might occur accidentally or because a low-lying excited state is energetically favorable for strong vibronic coupling, a "dynamic" epr spectrum may result, above a certain temperature, from populating higher vibronic levels of the complex.

(1) Abstracted from the Ph.D. thesis of J. Pradilla-Sorzano, Case Western Reserve University, 1972.

(2) Part V: J. Pradilla-Sorzano and J. P. Fackler, Jr., *Inorg. Chem.*, **12**, 1174 (1973).

(3) A general review on Jahn-Teller systems is given by M. D. Sturge, *Solid State Phys.*, **20**, 91 (1967).

(4) D. W. Smith, *J. Chem. Soc. A*, 1498 (1970).

(5) H. Elliot, B. J. Hathaway, and R. C. Slade, *Inorg. Chem.*, **5**, 669 (1966).

(6) T. S. Davis, J. P. Fackler, and M. J. Weeks, *Inorg. Chem.*, **7**, 1994 (1968).

(7) F. S. Ham, *Phys. Rev.*, **166**, 307 (1968).

(8) R. G. Wilson, F. Holuj, and N. E. Hedgecock, *Phys. Rev. B*, **1**, 3609 (1970).

(9) T. S. Piper and A. G. Karipides, *Inorg. Chem.*, **4**, 923 (1965).

(10) H. C. Allen, G. F. Kokoszka, and R. G. Inskeep, *J. Amer. Chem. Soc.*, **86**, 1023 (1964).

(11) A. D. Liehr and C. J. Ballhausen, *Ann. Phys. (New York)*, **3**, 304 (1958).

(12) R. H. Borcherts, H. Kanzaki, and H. Abe, *Phys. Rev. B*, **2**, 23 (1970).

(13) B. Bleaney, K. D. Bowers, and R. S. Trenam, *Proc. Roy. Soc., Ser. A*, **228**, 157 (1955).

(14) M. C. M. O'Brien, *Proc. Roy. Soc., Ser. A*, **281**, 323 (1964).

Temperature dependence has been observed in the spin-Hamiltonian parameters of a  $d^9$  ion in a tetragonal crystal field for Cu(II) doped into barium zinc formate tetrahydrate,<sup>15</sup> as well as Cu(II)-doped tris(phenanthroline)zinc(II) nitrate dihydrate.<sup>16</sup> The variation observed has been interpreted in terms of vibronic mixing of the upper  $d_{z^2}$  level into the  $d_{x^2-y^2}$  ground state. Here we report the results that have been obtained from single-crystal epr studies of Cu(II)-doped bis(hexafluoroacetylacetonato)bis(pyridine)zinc(II),  $\text{Cu-Zn}(\text{F}_6\text{acac})_2(\text{py})_2$ , at various temperatures between 4 and 300°K. Detailed crystal structures of the zinc and copper complexes were reported previously.<sup>2</sup>

### Experimental Section

Suitable crystals were grown from solutions which contained a copper-to-zinc mole ratio of 1:50 or 1:20 by using the method reported in part V.<sup>2</sup> Crystals which were grown from a mixture of  $\text{CCl}_4$  and  $\text{CH}_2\text{Cl}_2$  are designated as the  $\alpha$  crystallographic form, and those obtained directly from pyridine solution have been labeled as the  $\beta$  crystallographic form. Unless the  $\beta$  form is explicitly specified, the experimental data will refer to the  $\alpha$  form.

Crystals obtained at the highest copper concentration were used for epr measurements at 4°K and polarized optical absorption studies. Most of the crystals were in the form of thick hexagonal plates with the side faces slightly inclined to the main 001 face (Figure 1). The "a" axis lies parallel to the long axis of the hexagonal plate which also contains the "b" axis. Some other crystals are cleaved along the "a" axis.

Dilute single crystals were oriented in a Weissenberg camera and then transferred to appropriate crystal holders. For room-temperature epr measurements the method described by Levy<sup>17</sup> and by Weeks and Fackler<sup>18</sup> was used. For measurements in the temperature range from 133 to 300°K the crystals were mounted on a quartz rod which was inserted in a Varian E-229 goniometer sample rotator. The epr data above 133°K were obtained at X band using a Varian E-3 spectrometer. The field sweep was calibrated using Ultramarine Blue<sup>19</sup> and vanadyl acetylacetonate<sup>20</sup> as standards. Polycrystalline DPPH was used as a "g" marker.

A superheterodyne spectrometer (X band) was used for recording epr data at liquid helium temperature. The crystals were mounted on polyethylene sheets which were attached on a wall of the microwave cavity. Measurements were made at 15 or 20° intervals by rotating the magnet. The klystron frequency was measured directly with a wavemeter and polycrystalline DPPH was used as a g marker.

Rotation data obtained at room temperature about the three mutually perpendicular axes  $a$ ,  $b$ , and  $c^*$  were fitted to expressions of the type given by Schonland<sup>21</sup> and Lund and Vanngard.<sup>22</sup> Diagonalization gave the eigenvalues and vectors for the "g" and hyperfine tensors. At 133°K the spectra were observed in planes normal to the "b" and "c\*" crystallographic axes. Since the directions of the tensor principal components were known, from room-temperature data, to lie on these planes, spectra were recorded for orientations in which maximum or minimum "g" and hyperfine values were found. In order to investigate the variation of the magnetic parameters, measurements were taken at various temperatures with the magnetic field along the "b" axis, as well as for dilute powder samples. The low-temperature (4.2°K) spectra were recorded at 15° rotation intervals in planes perpendicular to the "b" and "a" axes. Rotation data about the "b" axis were fitted to expressions of the type given by Schonland<sup>21</sup> and maximum and minimum "g" and hyperfine values were calculated.

Polarized optical absorption spectra in the region 5000–21,000  $\text{cm}^{-1}$  were taken in dilute crystals of the copper complex (5 and 2%)

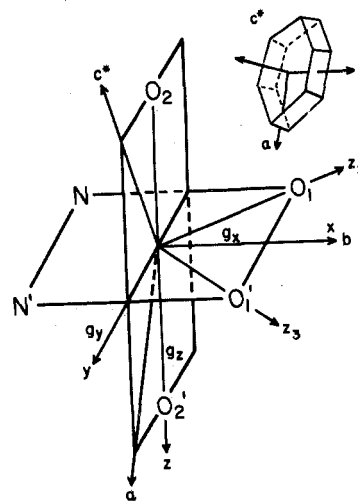


Figure 1. Relative positions of the molecule and its magnetic tensors with respect to the axes and faces of the crystal.

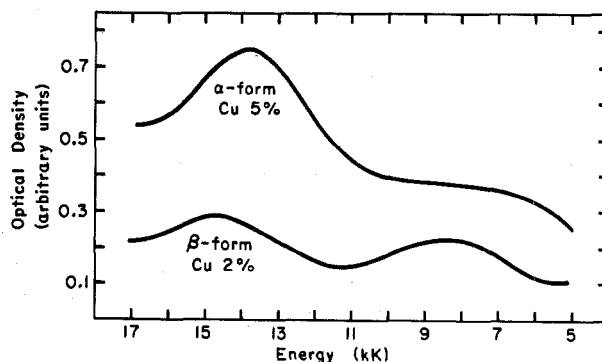


Figure 2. Single-crystal electronic spectra at 77°K for Cu-doped  $\text{Zn}(\text{F}_6\text{acac})_2(\text{py})_2$ ,  $\alpha$  and  $\beta$  crystallographic forms.

for both  $\alpha$  and  $\beta$  crystallographic forms with a Cary 14 spectrometer. Polarized light with the electric vector parallel to the largest crystal faces was used. The dewar and the polarizers described by Davis<sup>23</sup> were used for measurements at room temperature and liquid nitrogen temperature.

### Results

**Electronic Spectra.** For single crystals of  $\text{Cu-Zn}(\text{F}_6\text{acac})_2(\text{py})_2$ , both  $\alpha$  and  $\beta$  crystallographic forms, two bands were found whose positions were invariant with temperature. None of these bands show spectral polarizations. Spectra at liquid nitrogen temperature are shown in Figure 2.

**Epr High-Temperature Spectra.** At temperatures above 133°K the epr spectra show that all molecules in the crystal are magnetically equivalent regardless of their relative orientation to the magnetic field. Hence, the spectrum could be studied without the complications that arise from overlapping spectra of nonequivalent ions in the unit cell. In Table I are given the principal values for the  $g$  and hyperfine tensors at 298 and 133°K, together with the direction angles for the magnetic principal axes relative to certain crystallographic axes. Also given are the calculated direction angles, relative to the crystallographic axes, for the vector directions  $\text{M-O}(1)$ ,  $\text{M-N}$ , and  $\text{M-O}(2)$  of the  $\text{Zn-Cu}(\text{F}_6\text{acac})_2(\text{py})_2$  molecule (Figure 1).

The magnetic data could be fitted to the usual spin Hamiltonian for  $S = 1/2$

$$\mathcal{H}_s = \beta(g_z H_z S_z + g_y H_y S_y + g_x H_x S_x) + A_z I_z S_z + A_y I_y S_y + A_x I_x S_x \quad (1)$$

(23) T. S. Davis, Ph.D. Thesis, Case Institute of Technology, Cleveland, Ohio, 1967.

(15) T. Ramasubba and R. Srinivasan, *Phys. Lett.*, **22**, 143 (1966).

(16) G. F. Kokoszka, C. W. Reimann, H. C. Allen, and G. Gordon, *Inorg. Chem.*, **6**, 1657 (1967).

(17) J. D. Levy, Ph.D. Thesis, Case Western Reserve University, 1971.

(18) M. J. Weeks and J. P. Fackler, *Inorg. Chem.*, **7**, 2548 (1968).

(19) D. M. Gardner and G. K. Fraenkel, *J. Amer. Chem. Soc.*, **77**, 6399 (1955).

(20) F. A. Walker, R. L. Carlin, and P. H. Reiger, *J. Chem. Phys.*, **45**, 4181 (1966).

(21) D. S. Schonland, *Proc. Phys. Soc., London*, **73**, 788 (1959).

(22) A. Lund and T. Vanngard, *J. Chem. Phys.*, **47**, 2979 (1965).

**Table I.** Principal Values and Axes for the  $g$  and Hyperfine Tensors at High Temperatures<sup>a</sup>

Vector	Value at		Direction angles, deg		
	298°	133°	<i>a</i>	<i>b</i>	<i>c</i> *
M-O(1)			112.8	40.8	121.8
M-N			112.1	130.5	131.4
M-O(2)			146.9	85.6	57.4
Equatorial plane <sup>d</sup>			32.5	90.0	122.5
Vertical plane <sup>d</sup>			67.5	44.9	53.5
$g_x$	2.113	2.075	90.0	0.0	90.0
$g_y$	2.116	2.081	46.45	90.0	43.2
$g_z$	2.278	2.337	43.25	90.0	133.2
$A_x$	(9) <sup>b</sup>	4 <sup>e</sup>	90.0	0.0	90.0
$A_y$	(23)	7	48.7	90.0	41.2
$A_z$	104	147 <sup>c</sup>	41.2	90.0	131.2
$(A_N)_z$		11 G			
$(A_N)_x$		13 G			

<sup>a</sup> Estimated errors for eigenvectors:  $g_y$  and  $A_y$ ,  $\pm 4^\circ$ ;  $g_z$  and  $A_z$ ,  $\pm 1^\circ$ ; eigenvalues:  $g_x$ ,  $g_y$ , and  $g_z$ ,  $\pm 0.001$ ;  $A_x$ ,  $\pm 1.0$ ;  $A_N$ ,  $\pm 0.5$  G. <sup>b</sup> Values in parentheses have been calculated by extrapolation. <sup>c</sup> Copper-63. <sup>d</sup> Vectors defined by least-squares planes through  $MN'O(1)O'(1)$  and  $MN'O(1)O(2)O'(2)$ , respectively. <sup>e</sup> Hyperfine parameters are given in  $10^{-4}$  cm<sup>-1</sup>.

This assumes that the  $g$  and  $A$  tensors have the same axis system. The small in-plane anisotropy of the  $g$  tensor could not be effectively resolved and the  $g_x$  direction was assumed to be coincident with the  $b$  axis, as required by the twofold molecular symmetry of the complex. On this basis, the hyperfine tensor was calculated. The agreement, within experimental error, between the values found for the direction angles for the principal components ( $z$  and  $y$ ) of the  $g$  and  $A$  tensors gives validity to this assumption. Otherwise, cross terms would have to be included in the expression of the spin Hamiltonian.

Agreement is found to be fair between the magnetic  $z$  direction and the normal to the least-squares plane through the  $(Zn,Cu)NN'O(1)O'(1)$  atoms of the molecule (equatorial plane). The dot product between the magnetic  $z$  axis and this normal vector shows that there is an angle of  $10^\circ 44'$  between these two directions. This result implies that the  $Cu^{2+}$  ion occupies a site in the doped crystal with an elongated tetragonal structure. The elongation is along the M-O(2) bond cis to both coordinated pyridine molecules. This is consistent with the structure found for  $Cu(F_6acac)_2(py)_2$  by X-ray diffraction.<sup>2</sup>

At room temperature the copper hyperfine structure was not resolvable in directions nearly parallel to the equatorial plane. Below about 170°K the superhyperfine structure was clearly observed for all directions. When the magnetic field is directed along the  $z$  magnetic axis, the superhyperfine structure is composed of five lines for transitions between copper spin states ( $m_I = 1/2$ ). The separation between superhyperfine lines is 10.5 ( $\pm 0.5$ ) G and is due to the interaction of two equivalent nitrogens. For transitions between copper spin states ( $m_I = 3/2$ ) two extra peaks are found at the highest and lowest field of the spectrum which we attribute to the interaction of <sup>65</sup>Cu. In the  $g_{\perp}$  band the superhyperfine structure is composed of six lines equally spaced ( $13.2 \pm 0.5$  G) when the field is directed along the " $b$ " axis (Figure 3). Along the  $y$  direction seven lines were found. Separations between these lines range from 13 to 8 G. Well-resolved spectra were also obtained in other directions near the equatorial plane with about 13-G superhyperfine splitting.

Because of the overlapping between the ligand and copper hyperfine transitions in the perpendicular spectrum, the copper parameters cannot be precisely measured. From the

**Table II.** Magnetic Parameters from Powder Spectra for  $\alpha$  and  $\beta$  Forms

$g'_{\parallel}$	$10^4 A'_{\parallel}$ , cm <sup>-1</sup>	$g'_{\perp}$	Temp, °K
$\alpha$ Powder			
2.279	113	2.117	297
2.297	118	2.102	283
2.304	123	2.098	273
2.311	128	2.092	253
2.325	143	2.082	213
2.340	144	2.073	133
$\beta$ Powder			
2.325	152	2.060	143

total width of the perpendicular components we have estimated the magnetic parameters  $A_x = 4$  and  $A_y = 7$  G. The hyperfine structure reported above also indicates that these parameters are less than the nitrogen hyperfine value  $A_{1N} = 13$  G, since eight lines would be expected for equal values of copper and nitrogen hyperfine parameters.

Both single-crystal and powder epr spectra show a temperature dependence for the magnetic parameters above 133°K. Those variations observed in the spectra of the  $\alpha$  form were reversible. In contrast, no temperature dependence was found for the epr parameters of Cu(II) doped into the  $\beta$  crystallographic form. The  $g$  and  $A$  hyperfine values obtained from diluted powder samples are listed in Table II.

**Epr Low-Temperature Spectra.** Measurements at 4.2°K show that at low temperature a transition takes place in the paramagnetic resonance spectrum. Instead of a single set of resonance lines, the spectrum is found to consist of three sets of lines. Two of these signals (indices 2 and 3) have equal values for their magnetic parameters and intensities. The other (index 1), which is the strongest one, corresponds to  $g$  and  $A$  tensors nearly equivalent to those found at 133°K. These data can be interpreted to indicate three separate kinds of cupric ions in the lattice, two of which are equivalent, having their principal magnetic axes ( $z_2$  and  $z_3$ ) symmetrically related by the twofold molecular axis (Figure 1).

The epr spectrum was examined in planes normal to the " $b$ " and " $a$ " axes of the crystal. In a direction normal to " $b$ " the spectrum of one ion, which gives rise to the strongest signal, is in the lowest field (highest  $g$  value,  $g_z(1) = 2.344$ ), and the other two coincide at a higher field, while at 90° from such direction one is in the highest field (lowest  $g$  value,  $g_y(1) = 2.09$ ) while the other two coincide at a lower field. Epr lines for rotation about " $b$ " are shown in Figure 4. The  $g_1$  tensor is coincident with the  $g$  tensor found at room temperature but the components of the  $g_2$  tensor,  $g_z(2)$  and  $g_y(2)$ , are about 20° apart from  $g_1$  in the  $zy$  plane. With the magnetic field along the " $b$ " axis the spectra are also found to consist of two sets of lines (Figure 5). The strongest signal is in the highest field ( $g_x(1) = 2.07$ ) while the other two coincide at lower field ( $g_x(2) = 2.23$ ). As the field is rotated away from the " $b$ " axis in the plane normal to the " $a$ " axis, the weakest signals move into lower field, reaching their maximum  $g$  values at an angle of about 45° from the " $b$ " axis. At this point the spectra of the two equivalent ions do not coincide; the weakest sets of lines are found at lowest field overlapping with the strongest set, which is centered in the highest field (Figure 6).

These results are consistent with a system of three magnetic tensors with the principal axis of each ion nearly lying along the metal-oxygen bonds of the Cu-doped molecule (Figure 1). The oxygens cis to the coordinated pyridines nearly define the principal magnetic axis ( $z$ ) which corre-

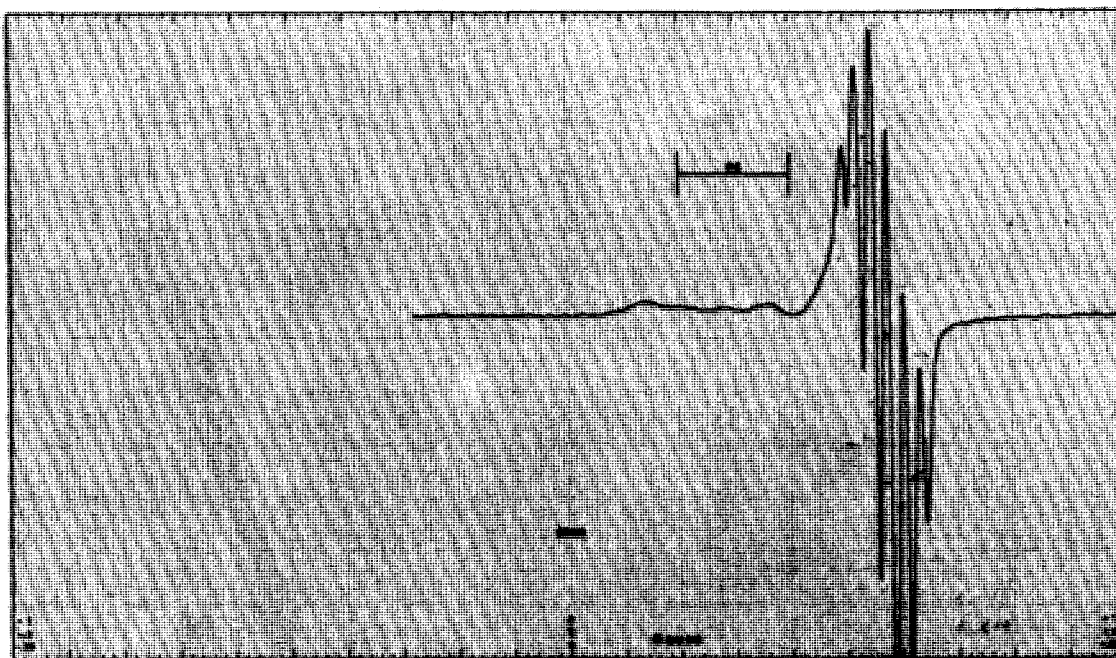


Figure 3. Single-crystal epr spectrum for  $\text{Cu-Zn}(\text{F}_6\text{acac})_2(\text{py})_2$  when the magnetic field is directed along the  $b$  axis ( $x$  direction) at  $133^\circ\text{K}$ .

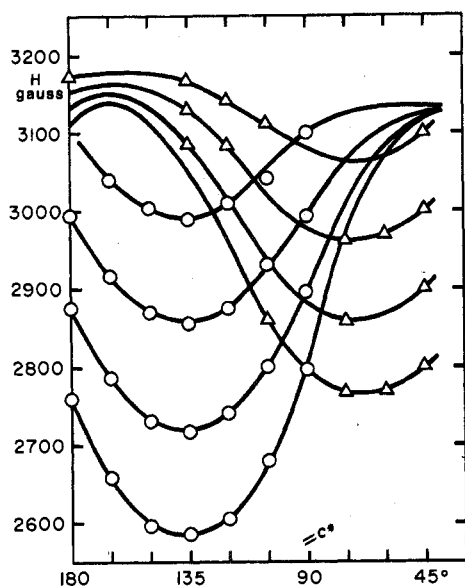


Figure 4. Epr lines recorded at  $4.2^\circ\text{K}$  for rotation about the  $b$  axis. Data points are marked with  $\circ$  and  $\Delta$  for configurations 1 and 2, respectively. Angles of rotation equal to 0 and  $90^\circ$  correspond to direction of the magnetic field parallel to the " $a$ " and " $c^*$ " directions, respectively. The resonance line for DPPH is at  $H = 3257 \text{ G}$ .

sponds to the strongest epr signal. The magnetic parameters and the direction angles for the magnetic principal axes for this ion (index 1) are listed in Table III, together with the calculated  $g$  and  $A$  values of the other two ions (indices 2 and 3) having their  $z$  axes defined by the oxygens trans to the coordinated pyridines. The principal  $g$  value ( $g_{\parallel}(2)$ ) for the equivalent tensors (2 and 3) was approximately evaluated by using the expressions

$$\overline{g_x(2)}^2 = \overline{g_{\parallel}(2)}^2 \cos^2 \alpha + \overline{g_{\perp}(2)}^2 \sin^2 \alpha$$

$$\overline{g_y(2)}^2 = \overline{g_{\parallel}(2)}^2 \cos^2 \alpha' + \overline{g_{\perp}(2)}^2 \sin^2 \alpha' \quad (2)$$

$$g_z(2) = g_{\perp}(2)$$

Table III. Principal Values and Axes for the  $g$  and Hyperfine Tensors at Low Temperature ( $4.2^\circ\text{K}$ )

Vector	Value	Estd error <sup>b</sup>	Direction angles, <sup>a</sup> deg		
			$a$	$b$	$c^*$
$g_x(1)$	2.070	$\pm 0.003$	90	0	90
$g_y(1)$	2.089	$\pm 0.003$	46	90	44
$g_z(1)$	2.344	$\pm 0.002$	44	90	134
$A_x(1)$	4		90	0	90
$A_y(1)$	(3.0) <sup>c</sup>	$\pm 2.5$	50	90	40
$A_z(1)$	151 <sup>d</sup>	$\pm 2.5$	40	90	130
$(A_N)_x(1)$	13.3 G	$\pm 0.5 \text{ G}$			
$g_x(2)$	2.226	$\pm 0.005$	90	0	90
$g_y(2)$	2.242	$\pm 0.004$	69	90	21
$g_z(2)$	2.074	$\pm 0.004$	21	90	111
$A_x(2)$	104 <sup>d</sup>	$\pm 3$	90	0	90
$A_y(2)$	107	$\pm 3$	65	90	25
$A_z(2)$	(12.5)	$\pm 3$	25	90	115
$g_{\parallel}(2)$	2.38	$\pm 0.01$			
$g_{\perp}(2)$	2.07	$\pm 0.01$			
$A_{\parallel}(2)$	140	$\pm 5$			
$A_{\perp}(2)$	(12)	$\pm 3$			

<sup>a</sup> Estimated error for direction angles is  $\pm 5^\circ$ . <sup>b</sup> Estimated error for the magnetic parameter was obtained from least-squares fitting to Schonland equations. <sup>c</sup> Values in parentheses were obtained by extrapolation. <sup>d</sup> Hyperfine parameters are given in  $10^{-4} \text{ cm}^{-1}$ .

where  $g_x(2)$ ,  $g_y(2)$ , and  $g_z(2)$  are the magnetic components found for the weakest epr signal along the directions shown in Table III. Angles  $\alpha$  and  $\alpha'$  are equal to approximately  $45^\circ$  and refer to the direction angles for the  $\text{M-O}(1)$  vector relative to the  $x(2)$  and  $y(2)$  magnetic directions, respectively (Tables I and III). Nearly equal experimental values for  $g_x(2)$  and  $g_y(2)$  suggest that the directions assumed for  $z_2$  and  $z_3$  are valid. The principal hyperfine values which have been calculated in a similar manner are listed in Table III.

Nitrogen superhyperfine structure was clearly shown in the perpendicular band of the strongest signal ( $A_N = 13.3 \text{ G}$ ). Because of the high modulation amplitude (10–20 G) used for recording the weakest set of lines, no information about the superhyperfine structure for these types of molecular configurations could be obtained. When the magnetic field was oriented along " $b$ ," the integrated intensities of the epr signals were in a ratio of about 5:1.

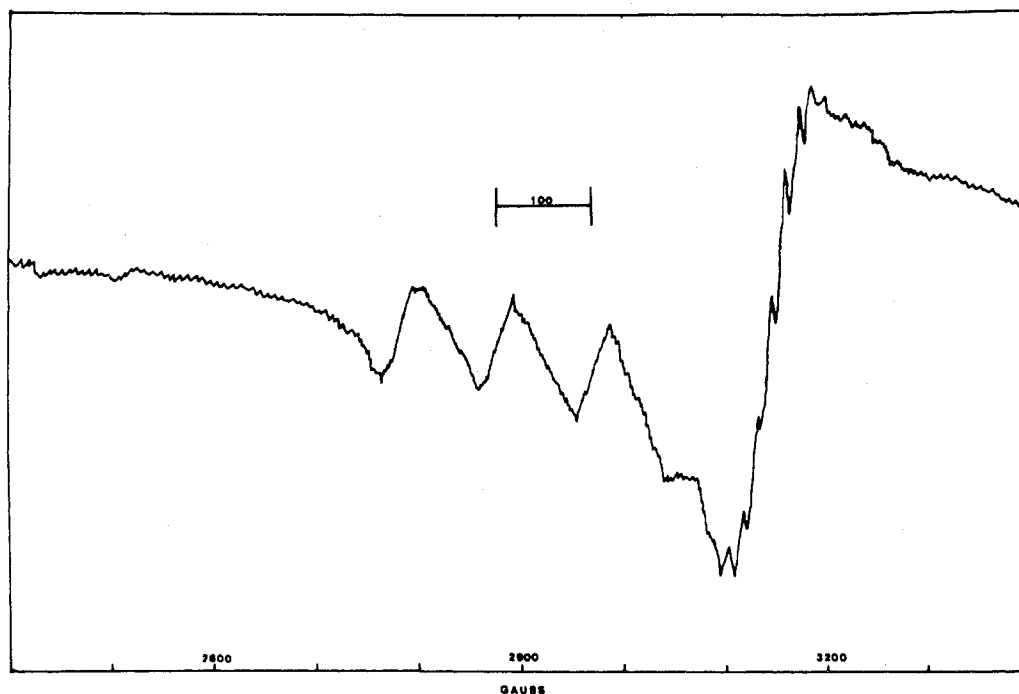


Figure 5. Epr spectrum at 4.2°K when the magnetic field is directed along the *b* axis.

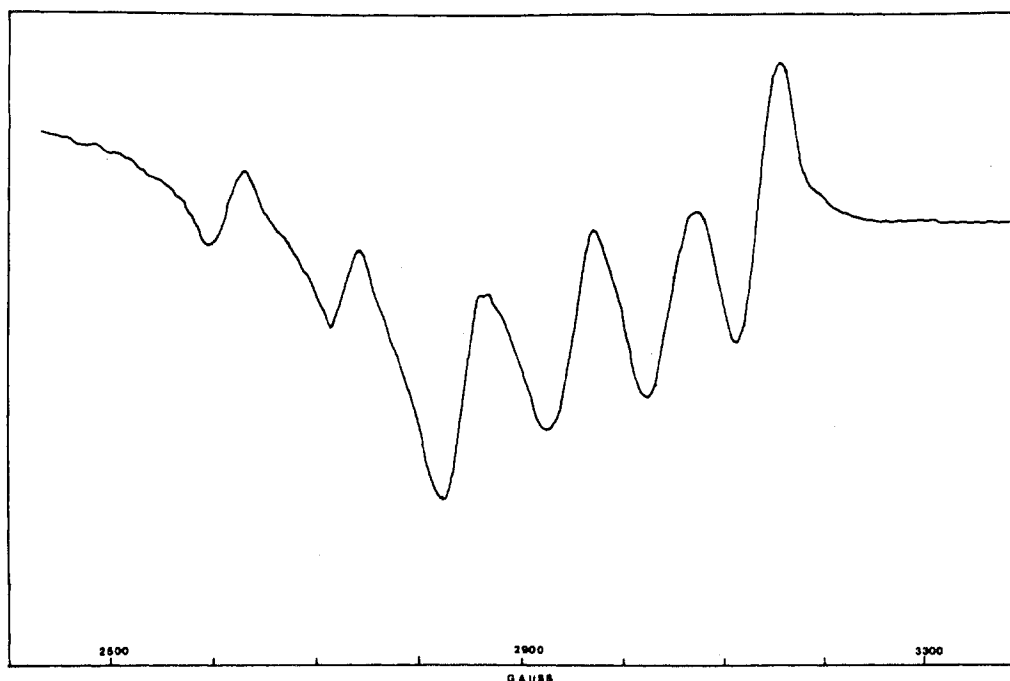


Figure 6. Epr spectrum at 4.2°K when the magnetic field direction is perpendicular to the "*a*" axis at about 45° between the "*b*" and "*c*" axes.

### Discussion

As already mentioned, for some "octahedral" copper complexes such as tris(phenanthroline)copper(II) and copper formate tetrahydrate, the temperature variation of the spin-Hamiltonian parameters has been explained as due to vibronic effects. The high-temperature epr spectrum of  $\text{Cu-Zn}(\text{F}_6\text{acac})_2(\text{py})_2$  exhibits a similar continuous variation over a large range of temperatures;  $g_{\perp}$  and  $A_{\perp}$  increase with temperature while  $g_{\parallel}$  and  $A_{\parallel}$  decrease.

The magnetic results are not paralleled by any significant shift, upon cooling, of the electronic transitions in the optical spectrum of  $\text{Cu-Zn}(\text{F}_6\text{acac})_2(\text{py})_2$ . Hence it is assumed

that the temperature dependence of the epr parameters indicates that this complex exhibits dynamic Jahn-Teller type distortions. Since the  $C_2$  symmetry of the molecule does not require degeneracy for the ground state, a low-lying excited state must be present which is capable of interacting under a vibrational mode with the ground state. Its energy must be comparable with the zero-point vibrational energy of the ground state in order that vibronic mixing takes place. The vibronic coupling can be accomplished by the B vibrational modes of the octahedron (formed by the ligand atoms) which have the appropriate symmetry for mixing the  $d_{z^2}$  orbital (A) into the  $d_{xy}$  (B) ground state. Evidence for this

interpretation is provided by the low-temperature epr spectrum which suggests three static distortions along the metal-oxygen bonds.

One useful aid to the understanding of the electronic-vibrational interaction in this system is shown in Figure 7. In this diagram, a one-dimensional space formed by the B mode of vibration of the octahedron is used for describing the relative energy of the three configurations.

It is well-known that the orbital doublet (E) ground state of the Cu(II) ion ( $d^9$ ) in a regular octahedral environment is usually split by a structural elongation along one axis of the octahedron. The energy of the system is described by a potential energy surface which has three minima corresponding to distortions along the metal-ligand bonds with generally only one of these minima being populated. In a few complexes these three minima are equally populated. Therefore the epr spectrum at low temperature should be the superposition of the spectra of different centers in the crystal corresponding to a random distribution among the equivalent distortions. The isotropic high-temperature spectrum is interpreted as arising from distortions which are rapidly traveling between the energy minima leading to an averaged  $g$  equal to  $1/3(g_{\parallel} + 2g_{\perp})$ .

We assume for the complex Cu-Zn( $F_6$ acac) $_2$  that a vibronic energy surface exists in which one of the three potential energy minima is slightly more favorable than the other two. In general this situation can be attained either by (1) internal strains which are imposed upon the paramagnetic defect by static distortions of the crystal environment or (2) the effect of external strain along one distortion axis. The resulting changes of the paramagnetic spectrum obviously depend on the molecular system as well as on the magnitude and direction of the applied strain.

Strain effects on the epr spectrum have been studied by Borcherts and coworkers.<sup>12</sup> They observed that the intensity of the parallel part of the spectrum of a stressed crystal of isolated Cu $^{2+}$  ion in NaCl increased relative to the perpendicular part. In this CuCl $^+$  complex, which has  $O_h$  symmetry, the axial strain applied causes a relative change in the ground-state energy of the three equivalent sites. For the system we have studied, an axially distorted molecule, the only energy minimum populated in the "unperturbed molecule" must be raised in energy relative to the other two minima by lattice forces, making the three minima nearly degenerate.

An interesting argument can be formulated that gives support to the above explanation for this pseudo Jahn-Teller phenomenon. Single-crystal optical spectra at liquid nitrogen temperature of Cu-Zn( $F_6$ acac) $_2$ (py) $_2$  show the presence of a low-energy band for both crystallographic forms ( $\alpha$  and  $\beta$ ). For the  $\beta$  form this band, found at 8500  $\text{cm}^{-1}$ , is well defined, while for the  $\alpha$  form the band found in the same region is very broad (Figure 2). This band can be assigned to the  ${}^2B(d_{xy}) \rightarrow {}^2A(d_{z^2})$  transition in accord with the E ground state. The d-d transition found at 14,700  $\text{cm}^{-1}$  for the  $\beta$  form is shifted about 900  $\text{cm}^{-1}$  to lower energy (13,800  $\text{cm}^{-1}$ ) for the  $\alpha$  form.

It has been pointed out by Davis, Fackler, and Weeks<sup>6</sup> that transitions between branches of the E ground state are particularly interesting in complexes for which regular octahedral configuration has been found. In the Frank-Condon approximation, transitions for molecules in various degrees of distortion are possible. Thus, in the spectra observed for octahedral molecules, there will be two major transitions as for permanently distorted molecules. However, for statically distorted molecules bands which are broad in the dy-

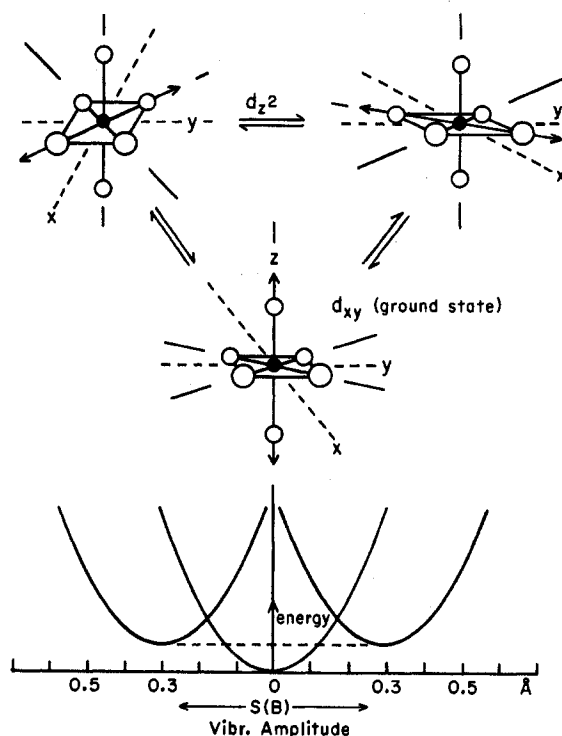


Figure 7. Vibronic energy diagram in a one-dimensional space of vibration. Three distorted configurations which correspond to the potential energy minima are shown.

amic case would sharpen up and shift to higher energies. Consequently, the significant shift in position of the d-d bands in going from the  $\beta$  to the  $\alpha$  form, as well as the exceptionally broad low-energy band found for the  $\alpha$  form, is further suggestive of the dynamic Jahn-Teller effect thought to be present in the  $\alpha$  form. In the  $\alpha$  form, the axially compressed host molecules (which have Zn-O bonds eclipsed throughout the unit cell) exert axial strain upon the copper complex, giving rise to a nearly degenerate Cu $^{2+}$  ground state. This result is consistent with the expected shift to lower energy of the d-d transitions for increasing axial coordination,<sup>24</sup> as well as the vibronic effects found in the epr and visible spectra.

In contrast to the behavior of the  $\alpha$  form of Cu-Zn( $F_6$ acac) $_2$ (py) $_2$ , the  $\beta$  crystallographic form exhibits epr parameters which are constant with temperature. Although the crystal structure of the  $\beta$  form is not known, single-crystal epr spectra indicate that the four molecules of the unit cell<sup>25</sup> are staggered. The similarity of the nitrogen hyperfine structure of the  $\alpha$  and  $\beta$  forms suggests a cis configuration for  $\beta$ -Cu-Zn( $F_6$ acac) $_2$ (py) $_2$ . Reference to Table II shows that the magnetic parameters found for the copper complex in the  $\beta$  form are similar to those found for the strongest signal for the  $\alpha$  form at low temperature. Higher  $g_{\parallel}$  values for the  $\alpha$  form are consistent with axial compression<sup>26</sup> in going from the  $\beta$  to the  $\alpha$  lattices.

**Pseudo Jahn-Teller Formalism.** The origin of the high-temperature epr spectrum in Cu-Zn( $F_6$ acac) $_2$ (py) $_2$  can be

(24) B. B. Wayland and A. F. Garito, *Inorg. Chem.*, **8**, 182 (1969).

(25) X-Ray photographs and density measurements for the  $\beta$  form indicate a monoclinic space group with four Cu-Zn( $F_6$ acac) $_2$ (py) $_2$  molecules and two extra pyridine molecules in the unit cell. Two epr signals are found for each arbitrary orientation. The nitrogen hyperfine structure is composed of five lines.

(26) S. Antosik, N. M. D. Brown, A. A. McConnell, and A. L. Porte, *J. Chem. Soc. A*, 545 (1969).

visualized as the "motional averaging" of the low-temperature spectra arising from transitions between different directions of distortion which become rapid relative to the microwave splitting.<sup>27</sup> If the "vibronic relaxation time"  $\tau_{ij} \gg 1/\Delta w_{ij}$ , when  $\Delta w_{ij} = (g_i - g_j)\beta H/\hbar$  for  $i, j = 1, 2, 3$ , three lines will be seen; if  $\tau_{ij} \ll 1/\Delta w_{ij}$ , only one line will be seen at an average  $g$  value ( $a_i g_i + a_j g_j$ ). The weighting coefficients  $a_{i,j}$  will follow the relative populations of the vibronic levels and  $\tau_{ij}$  the Arrhenius equation

$$\tau_{ij} = (\tau_{ij})_0 \exp(V_{ij}/kT) \quad (3)$$

where  $V_{ij}$  stands for the height of the potential barrier separating different directions of distortion. Presumably, transitions between energetically equivalent configurations, 2 and 3, occur faster for a given temperature than those involving the ground state.

Although the properties of  $\text{Cu-Zn}(\text{F}_6\text{acac})_2(\text{py})_2$  between 4.2 and 133°K have not been studied, the variation of the  $g$  values with temperature can be predicted from the  $g$  values of the three static configurations at low temperature by assuming that two processes occur as the temperature is raised: (1) an averaging of the two equivalent configurations to only one line at

$$g_{d_{z^2}} = (g_2 + g_3)/2 \quad (4)$$

and (2) a mixing of configuration 1 with the average obtained above to a final line at

$$g = b g_{d_{z^2}} + (1-b)g_1 \quad (5)$$

If we express the  $g$  tensors of the static complexes in a coordinate system given by the principal directions of the  $g$  tensor found at high temperature, we get on averaging

$$g'_{\parallel} = b g'_z(2) + (1-b)g'_z(1) \quad (6)$$

$$g'_{\perp} = b g'_{x,y}(2) + (1-b)g'_{x,y}(1)$$

Eliminating the temperature-dependent coefficient  $b$

$$g'_{\perp} = \alpha + \beta g'_{\parallel} \quad (7)$$

where

$$\alpha = g'_{x,y}(1) - g'_z(1)$$

$$\beta = \frac{g'_{x,y}(2) - g'_{x,y}(1)}{g'_z(1) - g'_z(2)}$$

$$g'_{x,y} = \frac{g'_x + g'_y}{2}$$

and where the primed quantities refer to the magnetic values along the principal directions of the tensor found at high temperature.<sup>28</sup> The results of these calculations are presented graphically in Figure 8, where the linear relationship between  $g'_{\perp}$  and  $g'_{\parallel}$  is shown. Values for the linear coefficients  $\alpha$  and  $\beta$  calculated from the low-temperature data and from a least-squares fit of the  $g$  values at different temperatures are close to confirming eq 7. Analogous expressions may hold for the hyperfine parameters; however, the situation is complicated by the unknown 4s orbital admixture into the ground state produced when mixing occurs with the  $d_{z^2}$  orbital.

A similar approximate expression

(27) H. M. McConnell, *J. Chem. Phys.*, **28**, 430 (1958).

(28) The  $g_{\perp}$  tensor is coincident with the  $g$  tensor found at room temperature but the components for the  $g_z$  tensor in the  $yz$  plane are about 20° apart from  $g_{\perp}$ . Consequently, the values  $g'_z(2)$  and  $g'_{x,y}(2)$  in eq 6 are different from the values  $g_z(2)$  and  $g_y(2)$  reported in Table III.

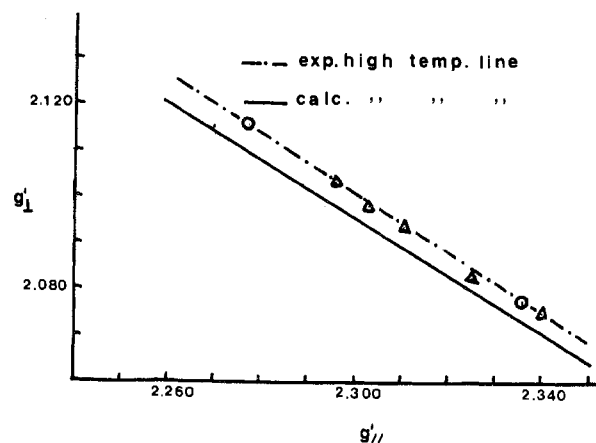


Figure 8. Linear equations for  $g'_{\perp}$  vs.  $g'_{\parallel}$  at different temperatures. Experimental values obtained from single-crystal spectra are marked with  $\circ$  and those for powder spectra with  $\Delta$ . Linear coefficients  $\alpha = 3.650 \pm 0.065$  and  $\beta = -0.674 \pm 0.028$  were obtained by a least-squares fit of the high-temperature spectra. For the equation obtained from the low-temperature data  $\alpha = 3.523 \pm 0.020$  and  $\beta = -0.616 \pm 0.020$ .

$$g = \cos^2\left(\frac{\phi_2}{2}\right) g_{x^2-y^2} + \sin^2\left(\frac{\phi_2}{2}\right) g_{3z^2-r^2} \quad (8)$$

has been proposed by O'Brien<sup>14</sup> for the dynamic Jahn-Teller effect in  $d^9$  ions with cubic symmetry. This equation arises when the excited state  $d_{z^2}$  is coupled with the  $d_{x^2-y^2}$  ground state by the E modes of vibration, *i.e.*

$$S_{2a} = q_2 \cos \phi_2$$

$$S_{2b} = q_2 \sin \phi_2 \quad (9)$$

$\phi_2$  being a function of time.

It is worthwhile pointing out that the pseudo Jahn-Teller case we have studied here follows the mathematical description predicted by Liehr<sup>29</sup> and Longuet-Higgins<sup>30</sup> on the basis of symmetry considerations. By using the permutations of the positions of any set of identical nuclei as symmetry operations for which the molecular Hamiltonian remains invariant, Liehr stated that any molecule whose permutational symmetry allows a " $C_3$ " subsymmetry will possess potential sheets similar to those of the simple trigonal symmetry  $X_3$  and  $YX_3$  molecules. However, for most molecules these permutational elements (which are not equivalent to rotations) need not be taken into account. These symmetry operations will be significant for stereochemically nonrigid molecules in which certain nuclear permutations can be achieved (no insuperable barriers). Permutation can have physical reality in cases where internal rotation is nearly free or can be brought about by a vibrational mechanism. In our  $\text{CuO}_4\text{N}_2$  system, permutation of the cis oxygen atoms in the trigonal  $\text{CuO}_3$  groups can be imagined.

In conclusion, it should be added that the present case, as well as other epr examples of pseudo Jahn-Teller systems,<sup>15,16</sup> although well established experimentally, is not yet understood in a complete manner. Modification of the theoretical treatment of the dynamic Jahn-Teller effect to accommodate the case of nonequivalent minima is needed.

Comparison between the magnetic parameters for  $\text{Cu-Zn-F}_6\text{acac})_2(\text{py})_2$  and those of some other base adducts of

(29) A. D. Liehr, *Progr. Inorg. Chem.*, **5**, 385 (1963).

(30) H. C. Longuet-Higgins, *Mol. Phys.*, **6**, 445 (1963).

$\text{Cu}(\text{F}_6\text{acac})_2$  will be given in another paper.<sup>31</sup> Interpretation of the molecular orbital coefficients and bonding parameters calculated by the methods of Kivelson and Nieman<sup>32</sup> and Swalen and coworkers<sup>33</sup> will be presented there.

(31) Part VII: J. Pradilla-Sorzano and J. P. Fackler, Jr., to be submitted for publication in *Inorg. Chem.*

(32) D. Kivelson and R. Neiman, *J. Chem. Phys.*, **35**, 149 (1961).

(33) J. D. Swalen, B. Johnson, and H. M. Gladney, *J. Chem. Phys.*, **52**, 4078 (1970).

Registry No. Copper, 7440-50-8;  $\text{Zn}(\text{F}_6\text{acac})_2(\text{py})_2$ , 38402-93-6.

**Acknowledgments.** This work was supported by the National Science Foundation, Grant GP-11701. Thanks are extended by J. P.-S. to the Lubrizol Foundation for an A. W. Smith Fellowship and the Colombian Institute "ICFES" for financial support. We also wish to thank Professor C. Y. Huang and Mr. Frederic J. Rackford of the Case Western Reserve University Physics Department for help with the He temperature epr measurements.

## Notes

Contribution from the Department of Chemistry,  
Southern Illinois University, Carbondale, Illinois 62901

### Electrochemical Generation and Spectral Characterization of the Bis(maleonitriledithiolato)nickel Trianion

Thomas E. Mines and William E. Geiger, Jr.\*

Received September 21, 1972

The oxidation-reduction behavior of metal-dithiolene complexes has attracted wide attention in the past decade and reports of complexes of the type  $\text{M}(\text{S}_2\text{C}_2\text{R}_2)_2^{n-}$  (I), where  $n = 0, 1, \text{ or } 2$ , have become commonplace.<sup>1,2</sup> It now appears certain that in most oxidation states of these complexes, molecular orbitals which are delocalized over the metal and ligands are responsible for their unusual electron-transfer properties. In the course of our electrochemical studies it has become apparent that the existence of more highly reduced complexes in this series, accessible at rather highly negative reduction potentials, has been overlooked. We report here the electrochemical generation and spectral characterization of the bis(maleonitriledithiolato)nickel trianion (I,  $\text{M} = \text{Ni}$ ,  $\text{R} = \text{CN}$ ,  $n = 3$ ),  $\text{NiMNT}^{3-}$ , in which the unpaired electron appears to be largely localized on the metal.

#### Experimental Section

The maleonitriledithiolate ligand and the  $\text{NiMNT}^{2-}$  complex were prepared by published methods.<sup>3</sup> ESR spectra were obtained on the Varian V-4502 spectrometer system employing 100-kHz field modulation and a 12-in. magnet. The Varian variable-temperature accessory was used to obtain spectra of frozen solutions, and diphenylpicrylhydrazyl (DPPH) served as a  $g$ -value reference. Optical spectra were obtained with the Beckman DK-1A spectrophotometer.

A Princeton Applied Research Model 173 potentiostat was employed in conjunction with a conventional ramp input and Hewlett-Packard Model 3300A function generator with Model 3302A trigger for polarographic and cyclic voltammetry experiments, respectively. Potentials are reported vs. the aqueous saturated calomel electrode (sce) and were monitored by a Simpson Model 2700 digital voltmeter. Data were read out with the Hewlett-Packard Model 7001A X-Y recorder or Tetronix Model 502A oscilloscope and camera. Cyclic voltammetry experiments were performed at

(1) J. A. McCleverty, *Progr. Inorg. Chem.*, **10**, 49 (1968).

(2) G. N. Shrauzer, *Accounts Chem. Res.*, **2**, 72 (1969).

(3) A. Davison and R. H. Holm, *Inorg. Syn.*, **10**, 11 (1967); E. Billig, R. Williams, I. Bernal, J. H. Waters, and H. B. Gray, *Inorg. Chem.*, **3**, 663 (1964).

the hanging mercury drop electrode. Other electrochemical techniques were conventional.

Spectrograde acetonitrile (Matheson Coleman and Bell) was dried over calcium hydride and kept under vacuum. Dimethoxyethane was dried with lithium aluminum hydride and distilled under vacuum onto either a potassium-anthracene mixture or lithium aluminum hydride. In a typical polarographic experiment, the solvent was distilled into a receiver flask and taken to a drybag where solutions were then prepared under a nitrogen atmosphere. Argon was used to purge residual oxygen from the solutions. The supporting electrolyte was tetrabutylammonium hexafluorophosphate, TBAHFP, obtained from Ozark Mahoning Co., recrystallized three times from 95% ethanol, and vacuum dried at 56°. Solutions were made 0.3 or 0.15  $M$  in TBAHFP with acetonitrile and dimethoxyethane, respectively, and approximately  $2 \times 10^{-4} M$  in  $\text{NiMNT}^{2-}$ . Controlled-potential electrolyses with the PAR 173 potentiostat were performed under vacuum at a mercury pool in a cell which employed the platinum quasireference electrode in a compartment separated from the bulk of the solution by a fine frit. Details of the cell construction will be reported elsewhere. Electrolyzed solutions were withdrawn and sealed under vacuum into a sample holder having a quartz cell for optical spectroscopy and an ESR sample tube.

#### Results and Discussion

We have studied the electrochemical reduction of  $\text{NiMNT}^{2-}$  by polarography and cyclic voltammetry (CV) at a mercury electrode<sup>4</sup> in acetonitrile and 1,2-dimethoxyethane solutions, and the pertinent data are collected in Tables I and II. Plots of  $-E$  vs.  $\log [i/(i_d - i)]$  from the polarographic data gave slopes close to that expected (59/ $n$  mV) for a reversible one-electron change, and the  $I$  values compared well with those obtained for the known reversible one-electron reduction<sup>5</sup> of the monoanion,  $\text{NiMNT}^-$ . The polarographic waves were diffusion controlled.

The invariance of the cyclic voltammetry cathodic half-peak potentials and cathodic current functions ( $i_{pc}/v^{1/2}$ ) with scan rate, as well as the unity ratio of anodic to cathodic peak currents, is diagnostic of reversible reductions uncomplicated by chemical reactions preceding or following the heterogeneous electron-transfer step.<sup>6</sup> Figure 1 shows a representative cyclic voltammogram.

$\text{NiMNT}^{3-}$  can be prepared from the dianion by controlled-potential electrolysis at a mercury pool, but the green solutions of the trianion are extremely air sensitive and revert to the orange color of the dianion upon exposure to even trace amounts of oxygen. We have not been successful in actual

(4) The reduction wave was also observed at a platinum working electrode.

(5) P. J. Lingane, *Inorg. Chem.*, **9**, 1162 (1970).

(6) R. S. Nicholson and I. Shain, *Anal. Chem.*, **36**, 706 (1964). Details of these measurements will be reported elsewhere.